Experimental and System-Level Simulation Study of Stick-Slip Characteristics in Pneumatic Cylinders

Hai Nguyen Ngoc , Phu Phung Pham , Bo Tran Xuan *

Posted Date: 2 April 2026

doi: 10.20944/preprints202604.0084.v1

Keywords: stick-slip; system modeling; friction model; pneumatic cylinder

 doi:10.20944/preprints202604.0084.v1

Article

Experimental and System-Level Simulation Study of Stick-Slip Characteristics in Pneumatic Cylinders

Hai Nguyen Ngoc [1,2], Phu Phung Pham [1] and Bo Tran Xuan [1,*]

[1] School of Mechanical Engineering, Hanoi University of Science and Technology, Hanoi 10000, Vietnam

[2] Faculty of Mechanical Engineering, Hanoi University of Civil Engineering, Hanoi 10000, Vietnam

* Correspondence: bo.tranxuan@hust.edu.vn; Tel.: +84-914-785386

Abstract

This paper presents a comprehensive experimental and simulation study on the stick–slip characteristics of pneumatic cylinders operating at low velocities. A pneumatic servo experimental system is constructed to systematically investigate stick–slip motion by measuring piston position, piston velocity, pressures in the two-cylinder chambers, and friction force. Extensive experiments are conducted on three pneumatic cylinders of different types and sizes to examine the influences of airflow rate, air source pressure, external load, and initial piston position on stick–slip behavior. Based on experimental observations, a complete mathematical model of the pneumatic servo system is developed. Unlike conventional approaches that simulate stick–slip motion using friction models driven solely by piston velocity, the proposed system-level model explicitly describes the entire dynamic process from valve control inputs to airflow, pressure evolution in the cylinder chambers, piston motion, and friction force. In addition, a new dynamic friction model is proposed by improving the revised LuGre friction model through the incorporation of a dwell-time-dependent static friction force, which is experimentally observed to play a critical role in governing stick–slip motion. Simulation studies are performed using both the proposed friction model and the revised LuGre friction model. The simulated results are systematically compared with experimental data for all tested cylinders. The results demonstrate that the proposed system model with the new friction formulation significantly improves the prediction of stick–slip characteristics, including the number of stick–slip cycles and the evolution of pressure and friction force, compared with conventional friction-model-based simulations.

Keywords: stick-slip; system modeling; friction model; pneumatic cylinder

1. Introduction

The stick–slip phenomenon, characterized by intermittent motion alternating between sticking and sliding phases, commonly occurs in mechanical systems operating under dry or mixed friction conditions, particularly in the negative-slope region of the Stribeck curve at low velocities [1–3]. In pneumatic actuation systems, stick–slip motion is frequently observed when pneumatic cylinders operate at low piston velocities or under low driving forces. This undesirable behavior leads to non-smooth motion, degradation of positioning accuracy, and accelerated wear of sealing components, which significantly limits the performance of pneumatic servo systems in precision applications [4–7].

To better understand and mitigate stick–slip motion in pneumatic cylinders, numerous experimental and analytical studies have been conducted. Tokashiki et al. [8] investigated stick–slip motion in pneumatic cylinders driven by meter-out circuits and identified the conditions for stick–slip occurrence using non-dimensional parameters. Zhang et al. [9] employed a neural network approach to predict the occurrence of stick–slip based on dynamic operating parameters. Fan et al. [10] analyzed stick–slip behavior in unsymmetrical pneumatic cylinders using dimensionless analysis, while Brun et al. [11] investigated the sticking and restarting phenomena and established necessary and sufficient conditions to suppress stick–slip motion. More recently, Azzi et al. [12]

 doi:10.20944/preprints202604.0084.v1

experimentally examined the influence of seal geometry and operating conditions on friction behavior, demonstrating that seal design plays a crucial role in the severity of stick–slip motion.

In parallel with experimental studies, significant efforts have been devoted to modeling stick–slip motion using friction models. Commonly used friction models, such as the Coulomb, Stribeck, Dahl, and LuGre models, describe friction force primarily as a function of the sliding velocity [3,13,14]. Among them, the LuGre model [14] and its extensions have been widely employed to simulate stick–slip motion due to their capability to represent presliding displacement and the Stribeck effect. Building upon the LuGre framework, Tran et al. [15] proposed a revised LuGre (RLG) friction model by incorporating dynamic lubrication film effects and hysteresis behavior. However, subsequent studies indicated that although the LuGre and RLG models can replicate certain aspects of stick–slip motion, their accuracy in reproducing experimentally observed stick–slip characteristics remains limited under low-velocity operating conditions, where system-level pneumatic dynamics become significant [16].

Although existing studies have significantly advanced the understanding of stick–slip phenomena in pneumatic cylinders, several fundamental limitations remain. Most previous research has primarily focused on developing or refining friction models and examining stick–slip behavior at the friction interface level, where the input to the friction model is typically limited to the piston velocity. In such approaches, the surrounding pneumatic system—including valve dynamics, airflow characteristics, air compressibility, and pressure evolution in the cylinder chambers—is often simplified or omitted. As a result, stick–slip motion is simulated without fully capturing the dynamic coupling between the control input at the valve level and the resulting mechanical response of the pneumatic cylinder.

Furthermore, although the dependence of static friction on dwell time has long been recognized as a key mechanism governing stick–slip motion [2], this effect is rarely incorporated into a complete system-level mathematical model of pneumatic servo systems. To the best of the authors' knowledge, no previous study has developed a comprehensive system model that starts from valve control signals and consistently describes the processes of airflow, pressure dynamics, cylinder motion, and friction evolution to simulate stick–slip characteristics of pneumatic cylinders under varying operating conditions. Consequently, there remains a lack of an integrated experimental and modeling framework capable of reliably predicting stick–slip behavior in pneumatic cylinders when multiple influencing factors are considered.

In this paper, the stick–slip characteristics of pneumatic cylinders are systematically investigated through combined experimental and simulation studies. This study focuses on the system-level mechanisms governing stick–slip motion in pneumatic cylinders, rather than on the detailed micromechanics of seal friction or valve internal flow structures. A pneumatic servo experimental system is constructed to measure piston position, piston velocity, chamber pressures, and friction force under the influence of cylinder type and size, airflow rate, air source pressure, external load, and initial piston position. Based on the experimental findings, a comprehensive mathematical model of the pneumatic servo system is developed, in which the entire dynamic process—from valve control input to cylinder motion—is explicitly modeled. In addition, a new dynamic friction model is proposed by improving the revised LuGre model through the incorporation of a dwell-time-dependent static friction force. Simulation results obtained using the proposed system-level model are validated against experimental data for three pneumatic cylinders, demonstrating significantly improved prediction of stick–slip characteristics compared with conventional friction-model-based approaches.

2. Experimental Test Setup

2.1. Experimental System

Figures 1 and 2 illustrate the experimental setup used to investigate the stick–slip characteristics of pneumatic cylinders. The experimental system consists of a double-acting pneumatic cylinder whose piston rod is connected to an external load. The load is supported by a linear guiding mechanism to ensure straight-line motion of the piston rod during operation. Airflow into and out of the two-cylinder chambers is controlled by two pneumatic proportional flow control valves (SMC,

 doi:10.20944/preprints202604.0084.v1

VEF3121-1-02), which independently regulate the motion of the piston. Each valve can deliver a maximum flow rate of 720 L/min.

The operating principle of the proportional flow control valves was as follows. When the control voltage $u_i (i = 1,2)$ was within the range of 0–2.5 V, the corresponding valve opened the exhaust port, allowing compressed air in the cylinder chamber to be discharged to the atmosphere. When the control voltage was within the range of 2.5–5 V, the valve supplied compressed air from the air source to the corresponding chamber. Based on these characteristics, the valve control strategy for the piston motion was defined by Equation (1). When the control signal $u > 0$, corresponding to the extending stroke, compressed air was supplied to the left chamber while the right chamber was exhausted. When $u < 0$, corresponding to the retracting stroke, compressed air was supplied to the right chamber while the left chamber was exhausted. When $u = 0$, no airflow was supplied to either chamber, and the piston remained stationary.

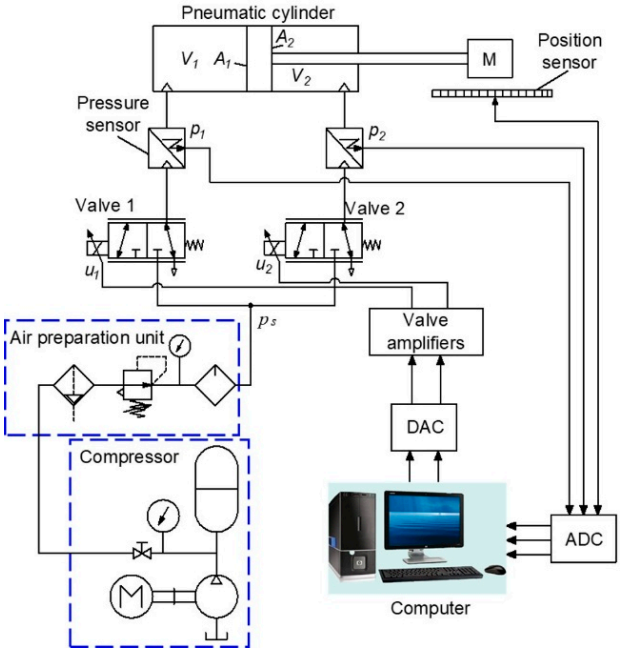

Figure 1. Schematic of the experimental test setup.

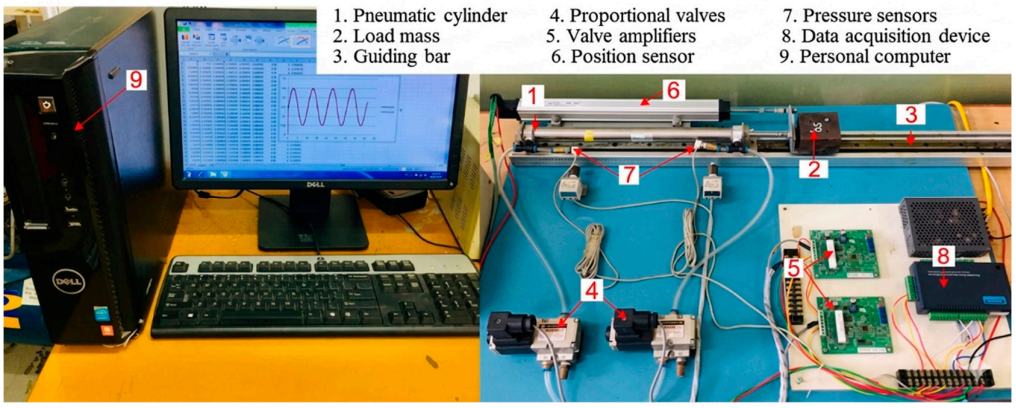

Figure 2. Schematic of the experimental test setup.

$$\begin{aligned} u_1 &= 2.5 + u \\ u_2 &= 2.5 - u \end{aligned} \tag{1}$$

 doi:10.20944/preprints202604.0084.v1

The piston position was measured using a linear position sensor (Novotechnik, LWH0300) with a measurement range of 300 mm and accuracy better than 0.5% of full scale. The sensor was mounted parallel to the cylinder using a dedicated mounting base. The pressures in the two-cylinder chambers were measured using two pressure sensors (SMC, PSE540A), each with a measurement range of 1 MPa and accuracy better than 1% of full scale. All sensor signals were transmitted to a personal computer through a 12-bit analog-to-digital converter (ADC). Control voltages were sent from the computer to the valve amplifiers via a 12-bit digital-to-analog converter (DAC). Both ADC and DAC functionalities were integrated into a single Advantech USB4711A data acquisition device. Experimental data acquisition and recording were performed at a sampling interval of 1.16 ms using Microsoft Visual C++ software. Compressed air was supplied by an air compressor connected through an air preparation unit to ensure stable supply pressure.

The stick–slip characteristics of the pneumatic cylinders were analyzed using piston position, piston velocity, pressures in the two-cylinder chambers, and friction force. The friction force F_r was estimated indirectly from the piston motion equation using the measured chamber pressures, piston acceleration, and load mass, as expressed in Equation (2). In this equation, A_1 and A_2 denote the effective piston areas of the two chambers, M represents the combined mass of the piston, piston rod, and external load, and a is the piston acceleration obtained by numerically differentiating the measured piston position. To reduce noise in the acceleration signal, an acausal first-order low-pass filter with a cutoff frequency of 32 Hz was applied. This indirect estimation method has been widely used in pneumatic system studies and provides sufficiently accurate friction characteristics for stick–slip analysis.

$$F_r = p_1 A_1 - p_2 A_2 - Ma \tag{2}$$

It should be noted that the friction force measured in the experimental system was not generated solely by the pneumatic cylinder. A portion of the total friction originated from the linear guiding mechanism supporting the piston rod during motion. Preliminary experiments indicated that the friction contribution from the guiding system accounted for approximately 10–15% of the total friction force. Compared with the friction produced by the cylinder seals, the guiding friction was relatively small and exhibited weak dependency on piston velocity. Therefore, in this study, the total friction force F_r estimated from Equation (2) was treated as an equivalent friction force acting on the piston. This representation was sufficient for capturing the dominant friction-induced stick–slip behavior, which was governed primarily by the friction characteristics inside the pneumatic cylinder.

All experiments were repeated multiple times under identical operating conditions, and consistent stick–slip characteristics were observed, indicating good repeatability of the experimental results.

2.2. Test Conditions

The experiments were designed to investigate the effects of key operating and system parameters on the stick–slip characteristics of pneumatic cylinders from a system-level perspective. The parameters under investigation included cylinder type and size, airflow rate, air source pressure, external load, and initial piston position. These parameters were selected because they directly influence airflow dynamics, pressure evolution, friction behavior, and piston motion in pneumatic servo systems.

a) Cylinder type and size: Three pneumatic cylinders manufactured by SMC, with different types and geometrical dimensions, were tested in this study. Their main specifications, including bore diameter, rod diameter, and stroke length, are summarized in Table 1. Due to practical availability, the tested cylinders differed simultaneously in both type and size. Rather than aiming at a statistical comparison between individual geometric parameters, this investigation focused on revealing how stick–slip characteristics vary across representative pneumatic cylinders with distinct structural properties. This approach allowed the robustness and applicability of the proposed system-level model to be evaluated across different cylinder configurations.

 doi:10.20944/preprints202604.0084.v1

Table 1. Specifications of tested pneumatic cylinders.

Parameters	Cylinder 1	Cylinder 2	Cylinder 3
Cylinder type	CM2L25-300Z	CDA2B0-200Z	MDBB3-200Z
Bore diameter (mm)	25	40	63
Rod diameter (mm)	10	16	20
Stroke (mm)	300	200	200

*b) **Airflow rate:*** The airflow rate supplied to the cylinder chambers was regulated by adjusting the control signals u_1 and u_2 of the proportional flow control valves according to Equation (1). The experiments were conducted under constant air source pressure and external load while varying the control signal u to examine the influence of airflow rate on stick–slip motion.

c) Air source pressure: The air source pressure was controlled via a pressure relief valve in the air preparation unit and varied from 3 to 7 bar, which lies within the typical operating range of pneumatic systems. During these experiments, the external load and valve control signals were kept constant to isolate the effect of supply pressure.

d) External load: Due to limitations of the experimental setup, the effect of external load was investigated only for the smallest cylinder (Cylinder 1). The load mass was varied up to a maximum value of 5.3 kg, while the air source pressure and valve control signals were maintained constantly. The purpose of this test was to examine the influence of inertia and load-induced friction on stick–slip behavior.

e) Initial piston position: The influence of initial piston position was investigated by starting the piston from different initial locations during the extending stroke. These experiments were performed under constant air source pressure, external load, and valve control signals to assess the effect of chamber volume on pressure buildup and stick–slip dynamics.

3. Mathematical Model of System

This section presents a system-level mathematical model of the pneumatic servo system developed to predict the stick–slip characteristics of pneumatic cylinders. Unlike conventional approaches that focus primarily on friction modeling with piston velocity as the main excitation, the proposed model explicitly describes the dynamic coupling between valve control input, airflow dynamics, pressure evolution in the cylinder chambers, piston motion, and friction behavior. Within this framework, stick–slip motion emerges naturally because of the interaction between pneumatic dynamics and friction-induced sticking–sliding transitions.

It is important to emphasize that stick–slip motion in pneumatic cylinders does not originate solely from friction characteristics. Previous studies have shown that air compressibility, pressure build-up and release processes, valve flow characteristics, and chamber volume variations play a crucial role in triggering stick–slip behavior through periodic energy accumulation and release, which interacts with friction forces during the sticking and sliding phases [8,11,13]. Therefore, accurate prediction of stick–slip motion requires a system-level model that consistently integrates pneumatic dynamics and friction behavior, rather than relying solely on friction models driven by piston velocity.

3.1. Modeling Assumptions

The pneumatic servo system exhibits strong nonlinear characteristics due to air compressibility, valve flow properties, and friction effects. To facilitate model development, the following assumptions are adopted, which are commonly used in pneumatic system modeling [11,13]:

i) the working fluid behaves as an ideal gas.
ii) air leakage in the cylinder chambers is neglected.

 doi:10.20944/preprints202604.0084.v1

iii) temperature variation in the chambers is negligible with respect to the supply temperature.
iv) pressure and temperature are spatially uniform within each chamber.
v) thermodynamic processes in the chambers are adiabatic.

These assumptions are standard in pneumatic system modeling and are suitable for capturing stick–slip dynamics.

3.2. Valve Flow Model

Based on the operating characteristics of the proportional flow control valves described in Section 2.1, the mass flow rate of air into or out of chamber $i(i = 1,2)$ is modeled as a function of the valve control voltage u_i, as expressed in Equation (3):

$$\dot{m}_i = \begin{cases} \gamma_{ib} p_s \sqrt{\frac{k}{RT_s}} K_{V1} \left(u_i - u_m\right) & ,u_m < u_i \le 5 \\ 0 & ,u_n \le u_i \le u_m \\ \gamma_{ie} p_i \sqrt{\frac{k}{RT_s}} K_{V2} \left(u_i - u_m\right) & ,0 \le u_i < u_n \end{cases} \tag{3}$$

where p_s denotes the supply pressure, p_i the chamber pressure, T_s the supply temperature, K_{V1} and K_{V2} the valve coefficients for intake and exhaust, respectively, u_m and u_n are the maximum and minimum voltages corresponding to the valve overlap; and γ_{ib} and γ_{ie} are dimensionless flow coefficients defined in Equations (4) and (5) as follows:

$$\gamma_{ib} = \begin{cases} \sqrt{\frac{2}{k-1}} \left(\frac{p_i}{p_s}\right)^{\frac{k+1}{2k}} \sqrt{\left(\frac{p_i}{p_s}\right)^{\frac{1-k}{k}} - 1}, & \frac{p_i}{p_s} \ge \left(\frac{2}{k+1}\right)^{\frac{k}{k-1}} \\ 0.58 & , \quad \frac{p_i}{p_s} < \left(\frac{2}{k+1}\right)^{\frac{k}{k-1}} \end{cases} \tag{4}$$

$$\gamma_{ie} = \begin{cases} \sqrt{\frac{2}{k-1}} \left(\frac{p_{atm}}{p_i}\right)^{\frac{k+1}{2k}} \sqrt{\left(\frac{p_{atm}}{p_i}\right)^{\frac{1-k}{k}} - 1} & , \frac{p_{atm}}{p_i} \ge \left(\frac{2}{k+1}\right)^{\frac{k}{k-1}} \\ 0.58 & , \frac{p_{atm}}{p_i} < \left(\frac{2}{k+1}\right)^{\frac{k}{k-1}} \end{cases} \tag{5}$$

where p_{atm} is the atmospheric pressure.

The formulation in Equation (3) establishes a direct link between the valve-level control input and the pneumatic dynamics of the system.

3.3. Chamber Pressure Dynamics

The pressure dynamics in the two-cylinder chambers are governed by continuity equations, which relate to the mass flow rate, chamber pressure, and piston velocity:

$$\begin{aligned} \dot{p}_1 &= \frac{k}{V_1} \left(RT_s \dot{m}_1 - p_1 A_1 v\right) \\ \dot{p}_2 &= \frac{k}{V_2} \left(RT_s \dot{m}_2 + p_2 A_2 v\right) \end{aligned} \tag{6}$$

where k is the adiabatic index, v is the piston velocity, and A_1, A_2 are the effective piston areas. V_1 and V_2 are the volumes of air in the cylinder chambers, expressed as functions of piston displacement x:

$$\begin{aligned} V_1 &= V_{10} + A_1 x \\ V_2 &= V_{20} + A_2 \left(L - x\right) \end{aligned} \tag{7}$$

 doi:10.20944/preprints202604.0084.v1

where L denotes the stroke length, and V_{10} and V_{20} are the dead volumes of chambers 1 and 2, respectively.

Equations (6) and (7) describe how air compressibility and chamber volume variation contribute to pressure build-up and release, which are essential mechanisms underlying stick–slip motion in pneumatic systems [8,11].

3.4. Piston Motion Equation

The equation of motion of the piston is formulated according to Newton's Second Law as follows:

$$Ma = p_1 A_1 - p_2 A_2 - F_r \tag{8}$$

where, F_r is the friction force in the pneumatic cylinder.

Through Equations (6)–(8), pneumatic energy stored due to air compression is periodically converted into mechanical motion, interacting with friction to produce sticking and sliding phases characteristic of stick–slip behavior.

3.5. Revised LuGre Friction Model

Friction plays a dominant role in stick-slip motion. Friction-induced instabilities have long been identified as fundamental causes of stick-slip behavior in mechanical systems [2,3,14]. Among various friction models, the LuGre model is widely adopted due to its ability to represent presliding displacement and the Stribeck effect [14]. To better capture the friction characteristics of pneumatic cylinders, Tran et al. proposed the revised LuGre (RLG) friction model, which incorporates hysteresis behavior and lubrication film dynamics [15,16]. In this study, the RLG friction model is adopted without altering its mathematical structure. Equations (9)–(15) are retained in their original form and describe the friction behavior of pneumatic cylinders. The friction force is expressed as:

$$F_r = F(z) + \sigma_1 \frac{dz}{dt} + \sigma_2 \left(v + T \frac{dv}{dt} \right) \tag{9}$$

$$\frac{dz}{dt} = v - \frac{F(z)}{g(v,h)} v \tag{10}$$

$$g(v,h) = F_c + \left[(1-h) F_s - F_c \right] e^{-(v/v_s)^n} \tag{11}$$

$$\frac{dh}{dt} = \frac{1}{\tau_h} (h_{ss} - h) \tag{12}$$

$$\tau_h = \begin{cases} \tau_{hp} & (v \neq 0, h \leq h_{ss}) \\ \tau_{hn} & (v \neq 0, h > h_{ss}) \\ \tau_{h0} & (v = 0) \end{cases} \tag{13}$$

$$h_{ss} = \begin{cases} K_f |v|^{2/3} & (|v| \leq |v_b|) \\ K_f |v_b|^{2/3} & (|v| > |v_b|) \end{cases} \tag{14}$$

$$K_f = (1 - F_c / F_s) |v_b|^{-2/3} \tag{15}$$

where $F(z)$ is the hysteresis function that simulates hysteresis behavior with nonlocal memory in the pre-sliding regime; z is the average deflection of the bristles, v is the relative velocity of piston; σ_1 and σ_2 are the micro-viscous friction coefficient and the viscous friction coefficient, respectively; T is the

 doi:10.20944/preprints202604.0084.v1

time constant for fluid dynamics; $g(v,h)$ is a Stribeck function; F_c is the Coulomb friction force; F_s is the static friction force; v_s is the Stribeck velocity; n is an appropriate exponent; h is the dimensionless lubricant film thickness; h_{ss} is the dimensionless steady-state lubricant film thickness parameter; K_f is the proportional constant for lubricant film thickness; v_b is the velocity within which the lubricant film thickness varies; τ_{hp}, τ_{hn} and τ_{h0} are the time constants for acceleration, deceleration, and dwell periods, respectively.

Despite its improved ability to represent hysteresis and lubrication effects, the RLG model assumes a constant static friction force, which constitutes a limitation when modeling stick–slip motion involving repeated sticking and sliding cycles.

3.6. Dwell-Time-Dependent Static Friction

In practical stick–slip motion, experimental observations show that the static friction force F_S evolves over successive cycles depending on the duration of the sticking phase, commonly referred to as the dwell time. This phenomenon has been identified as a key mechanism governing stick–slip behavior [2]. This effect is clearly confirmed by the experimental results obtained in the present study. Figure 3a shows the measured friction force during repeated stick–slip cycles for Cylinder 2. For each cycle, the static friction force $F_{s,i}$ is identified as the maximum friction force immediately before the onset of sliding, while the corresponding dwell time $t_{D,i}$ is defined as the duration during which the piston remains stationary between two successive slip events. As shown in Figure 3b, the static friction force increases with dwell time and follows an exponential-type trend.

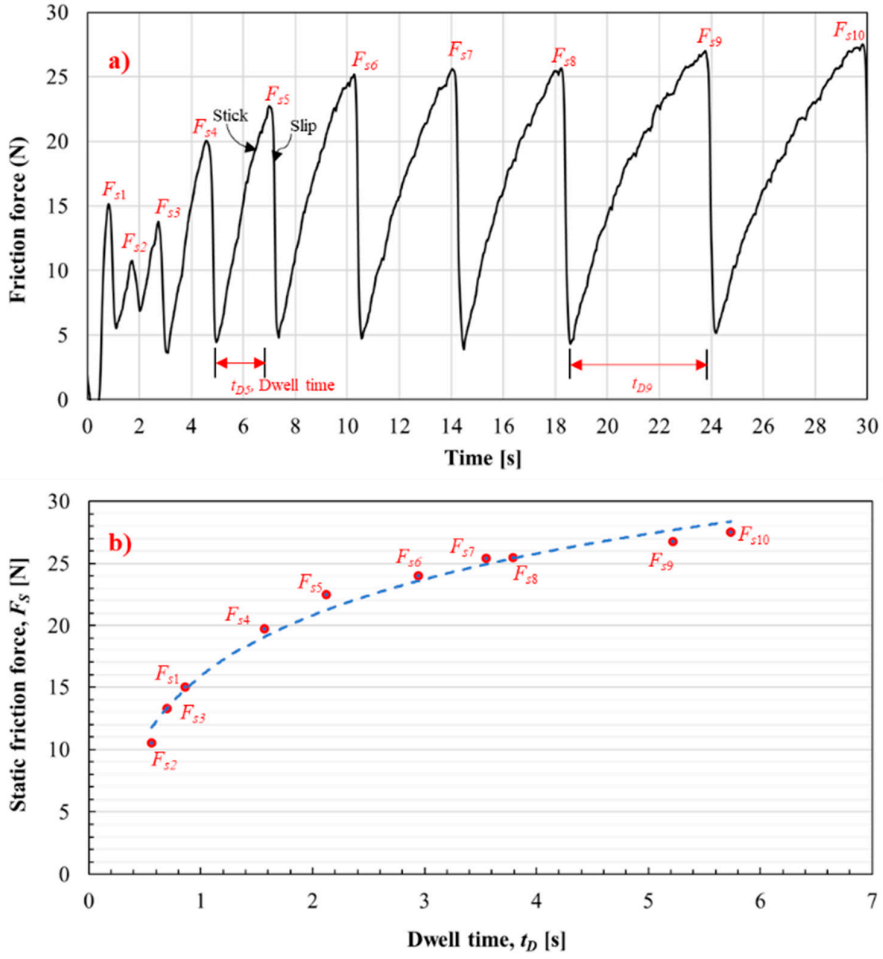

Figure 3. Determining the variation in static friction force of cylinder 2 with Dwell time: a) Friction force characteristics; b) Static friction force versus Dwell time.

 doi:10.20944/preprints202604.0084.v1

Motivated by this experimental evidence, the assumption of constant static friction in the RLG model is relaxed, and the static friction force is allowed to vary as a function of dwell time:

$$F_s\left(t_D\right) = F_{s\max} - \left(F_{s\max} - F_c\right)\exp(-\gamma t_D^{\alpha}) \tag{16}$$

where F_{smax} is the maximum static friction force achieved when the piston maintains a stick state for a significant amount of time; α and γ are empirical parameters. The parameters $F_{s\max}$, α, and γ characterize the friction properties of the pneumatic cylinder and are identified offline by curve fitting with the experimental characteristic curve of the static friction force versus dwell time. The proposed dwell-time-dependent formulation of static friction is empirical in nature and is intended to capture experimentally observed behavior within the operating time scales relevant to pneumatic stick–slip motion. During system-level simulation, the dwell time t_D is computed online as a natural outcome of the coupled pneumatic and mechanical dynamics: the dwell time is initiated when the piston velocity becomes zero and increases while the piston remains stationary under pressure build-up. Once sliding occurs, the dwell time is reset, and the corresponding static friction force is updated according to Equation (16).

Consequently, the structure of the RLG friction model is fully preserved, and Equation (16) represents a physically motivated extension, grounded in experimental observations, and embedded consistently within the complete pneumatic servo system model.

4. Results and Discussion

4.1. Experimental System

4.1.1. Stick-Slip Characteristics

Figures 4–6 present the experimentally measured piston position, piston velocity, pressures in the two-cylinder chambers, and friction force for the three tested pneumatic cylinders operating at low velocities. For all cylinders, the piston motion exhibits a stick–slip-type behavior characterized by alternating phases of nearly stationary motion and short slipping events. However, the temporal characteristics of these phases and the magnitude of the slip vary markedly among the cylinders.

For Cylinder 1 (Figure 4), the stick–slip motion is clearly pronounced. The piston remains stationary for a relatively long dwell time, on the order of several seconds, before a distinct slipping event occurs. Prior to each slip, the pressure in the driving chamber increases gradually and the friction force reaches a clear peak, approximately 15 N in the first cycle. Once sliding starts, the piston moves over a noticeable distance, accompanied by a rapid pressure drop, after which the piston stops again and a new stick–slip cycle begins. Subsequent cycles exhibit shorter dwell times and progressively smaller friction peaks.

Cylinder 2 (Figure 5) shows an intermediate behavior. Stick–slip motion is still evident, but the dwell times are generally shorter than those of Cylinder 1, and the piston exhibits smaller slip distances. In addition, slight continuous motion or creep can be observed during some sticking phases, indicating a transitional behavior between pronounced stick–slip and smoother motion. In contrast, Cylinder 3 (Figure 6) exhibits a fundamentally different quantitative characteristic. Although it has the largest bore diameter and piston area, it undergoes a significantly larger number of stick–slip cycles, each associated with very short dwell times and extremely small slip displacements. In this case, the piston starts to move after only a small pressure increase, but even a minimal displacement leads to a rapid expansion of the chamber volume and an immediate pressure drop. Consequently, the piston stops almost immediately after slipping, and pressure starts to build up again, resulting in frequent and rapidly repeated stick–slip cycles.

These observations demonstrate that stick–slip behavior in pneumatic cylinders cannot be interpreted solely based on chamber volume or cylinder size. Instead, it is governed by the coupled system-level interaction between piston area, chamber volume variation, pressure build-up rate, and friction characteristics. A large piston area reduces the pressure required to overcome static friction, while a rapid increase in chamber volume during motion leads to a fast pressure drop and early arrest

 doi:10.20944/preprints202604.0084.v1

of the piston. The balance between these effects determines the dwell time, number of cycles, and slip amplitude. These experimental results provide strong evidence that stick–slip motion is controlled by a nonlinear feedback mechanism involving pneumatic dynamics and mechanical response, thereby justifying the system-level modeling approach developed in Section 3.

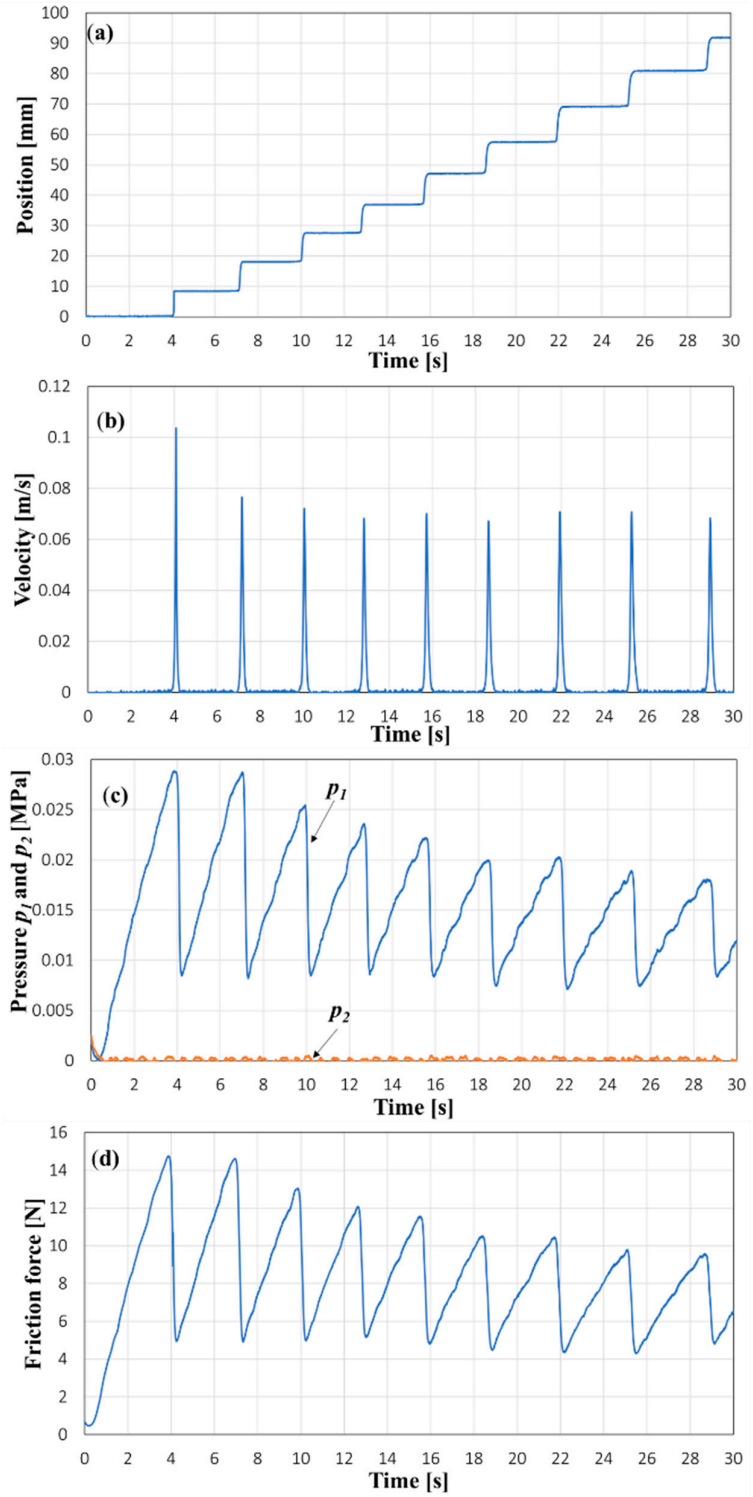

Figure 4. Stick-slip characteristics of the cylinder 1 (u = 0.29 V, p_s = 4 bar, M = 0.2 kg) (a) piston position, (b) piston velocity, (c) pressures in the cylinder chamber, (d) friction force.

 doi:10.20944/preprints202604.0084.v1

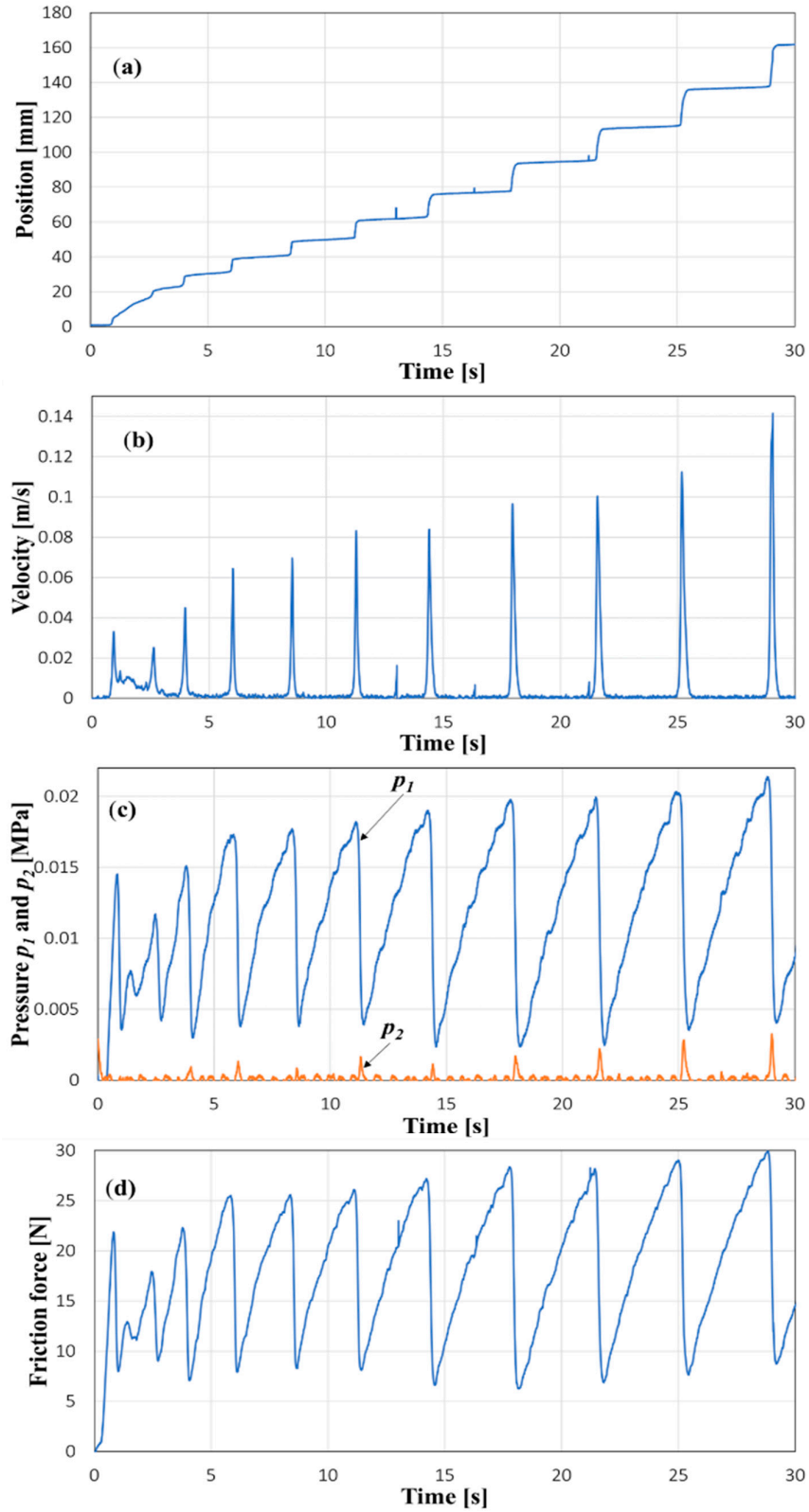

Figure 5. Stick-slip characteristics of cylinder 2 (u = 0.34 V, p_s = 4 bar, M = 0.2 kg): (a) piston position, (b) piston velocity, (c) pressures in the cylinder chamber, (d) friction force.

 doi:10.20944/preprints202604.0084.v1

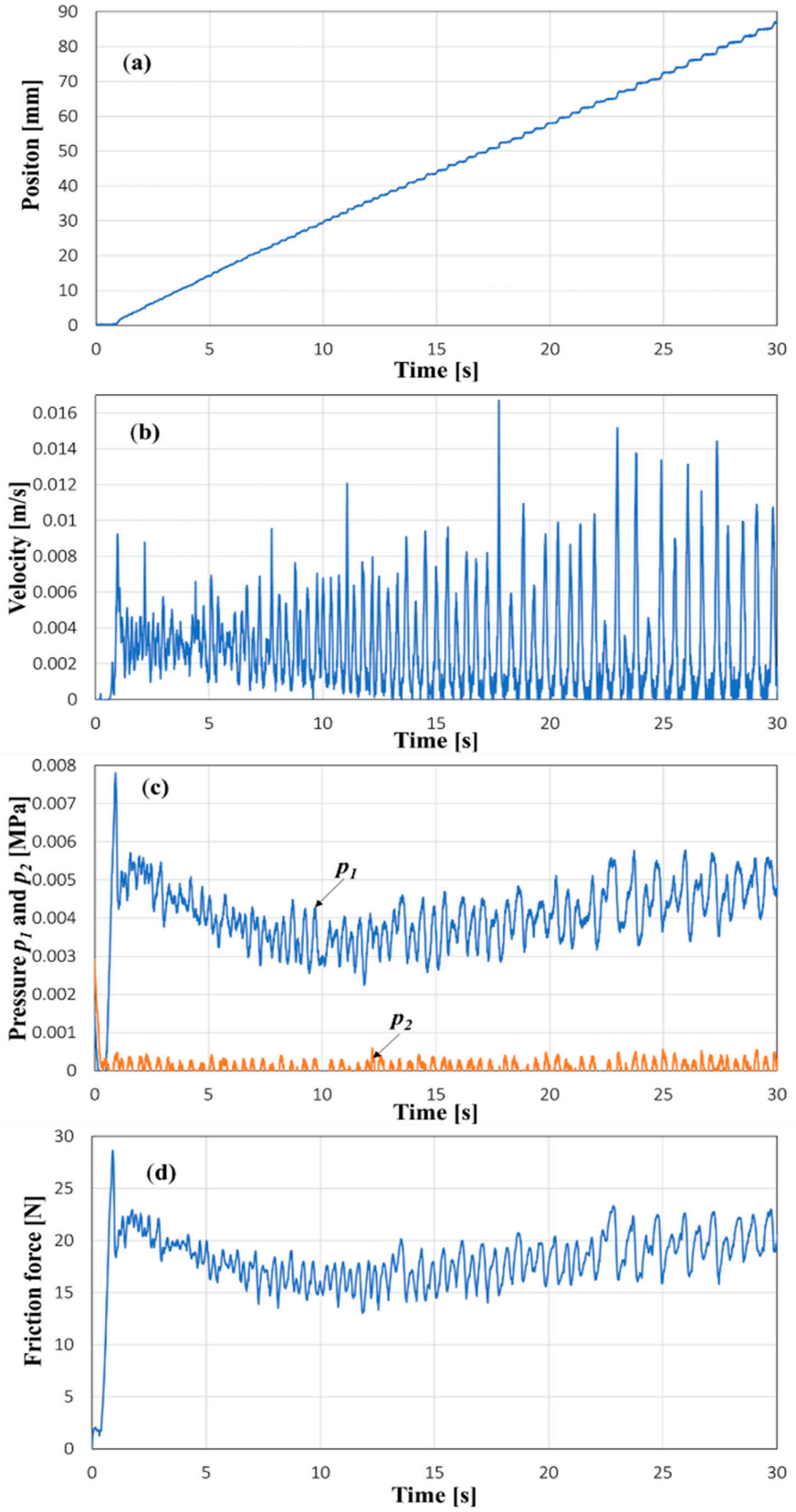

Figure 6. Stick-slip characteristics of the cylinder 3 (u = 0.32 V, p_s = 4 bar, M = 0.2 kg): (a) piston position, (b) piston velocity, (c) pressures in the cylinder chamber, (d) friction force.

 doi:10.20944/preprints202604.0084.v1

4.1.2. Effects of Airflow Rate

Figure 7 illustrates the influence of airflow rate on piston motion for the three pneumatic cylinders by varying the valve control signal u. Within the investigated range of airflow rates, increasing u leads to a pronounced reduction in the number of stick–slip events and a substantial decrease in the total time required for the piston to complete its stroke. However, the experimental results also reveal that the effect of airflow rate on stick–slip motion is gradual and cylinder-dependent, rather than representing an abrupt transition to fully continuous sliding.

At relatively low airflow rates (e.g., u = 0.28–0.29 V for Cylinder 1), the piston motion exhibits a clear step-like profile, characterized by long sticking phases followed by short slipping events. As the airflow rate increases to intermediate values, the dwell time of each sticking phase becomes shorter and the slip amplitude increases, resulting in a mixed motion regime in which brief sticking and partial sliding occur alternately. In this transitional regime, the step-like structure of the displacement curves becomes less pronounced but does not disappear entirely.

At the highest airflow rates examined in the experiments, the piston motion becomes significantly smoother and the stick–slip pattern is strongly attenuated. For Cylinders 1 and 2, the displacement curves approach a quasi-continuous behavior, whereas for Cylinder 3, small step-like features can still be observed, indicating residual micro stick–slip motion even at relatively high airflow rates. These observations suggest that, within the experimental airflow range, complete suppression of stick–slip motion may not be fully achieved for all cylinder geometries.

From a physical standpoint, increasing the airflow rate accelerates the rate of pressure build-up during the sticking phase, thereby reducing the dwell time required to overcome static friction. At the same time, higher airflow allows pressure to recover more rapidly after a slipping event, promoting smoother motion. The observed transition from pronounced stick–slip to strongly attenuated stick–slip therefore reflects a gradual shift in the balance between pressure build-up, pressure drop due to chamber volume expansion, and friction resistance. These results demonstrate that airflow rate governs not only the frequency of stick–slip cycles but also the qualitative nature of the piston motion within the experimentally investigated range.

4.1.3. Effects of Air Source Pressure

Figure 8 illustrates the influence of air source pressure p_s on the piston motion of the three pneumatic cylinders, with p_s varied from approximately 3 bar to 7 bar. This pressure range corresponds to typical operating conditions of pneumatic servo systems and represents the practical limit of the experimental setup used in this study. Within this investigated range, increasing the supply pressure leads to a significant reduction in the total motion time and a clear attenuation of stick–slip behavior for all three cylinders.

At lower supply pressures (e.g., p_s = 3–4 bar), the piston motion exhibits pronounced step-like characteristics, with relatively long dwell times and clearly separated slipping events. As the supply pressure increases, the step heights become larger and the dwell times associated with each sticking phase decrease, resulting in smoother overall motion trajectories. However, even at the highest supply pressures examined (p_s = 6–7 bar), small step-like features can still be observed, especially for Cylinder 3, indicating that micro stick–slip behavior persists within the tested pressure range.

It should be emphasized that the supply pressure does not act directly on the piston, since compressed air is first regulated by the proportional flow control valves before entering the cylinder chambers. An increase in supply pressure therefore affects piston motion indirectly by increasing the airflow rate delivered to the chamber for a given valve control signal. This higher airflow accelerates the rate of pressure build-up during the sticking phase, thereby reducing the dwell time before the pressure force becomes sufficient to overcome static friction and initiate sliding.

 doi:10.20944/preprints202604.0084.v1

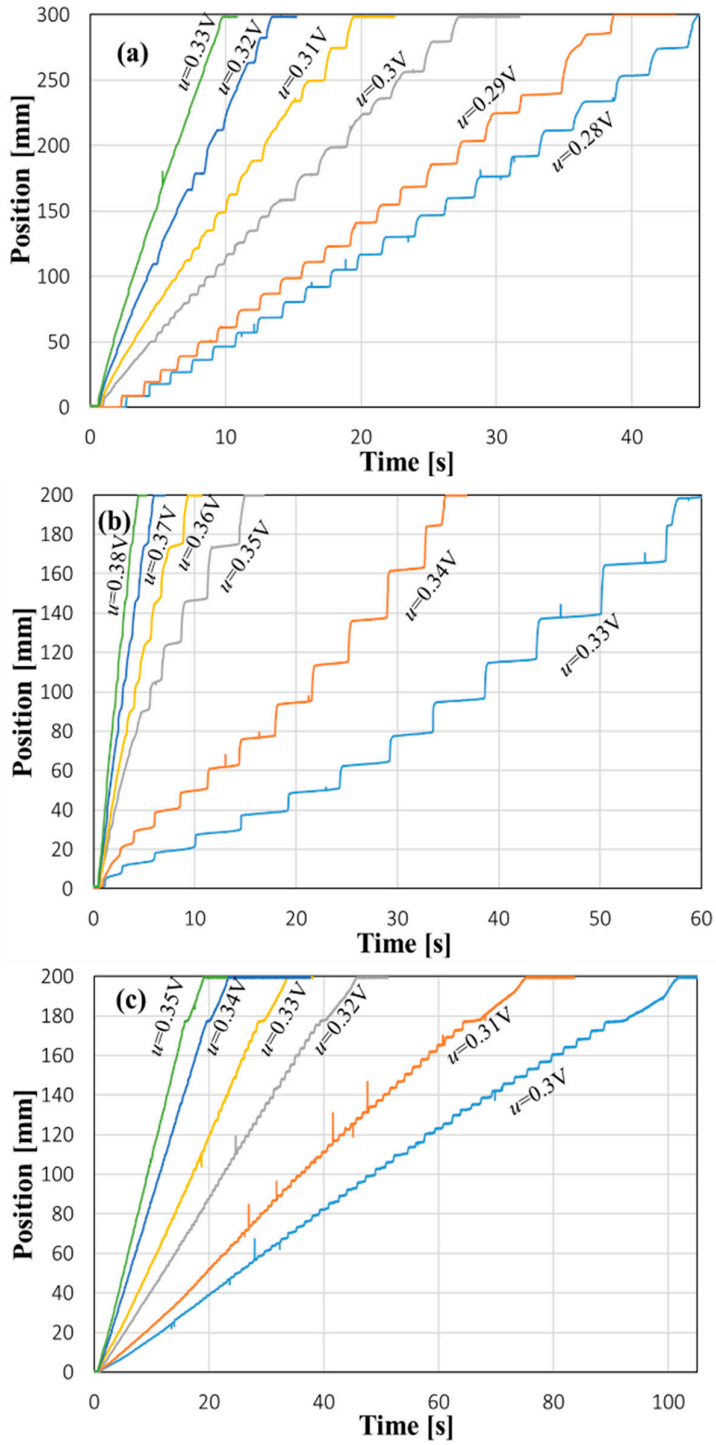

Figure 7. Effects of airflow rate on stick-slip motion (outstroke): a) cylinder 1, b) cylinder 2, c) cylinder 3.

Nevertheless, due to air compressibility and the rapid expansion of the chamber volume during slipping, the chamber pressure can still drop significantly after motion begins, causing the piston to stop again and leading to repeated stick–slip cycles. The persistence of residual stick–slip behavior at higher supply pressures, particularly for cylinders with large piston areas, indicates that within the practical operating pressure range investigated, increasing p_s alone is insufficient to completely eliminate stick–slip motion.

 doi:10.20944/preprints202604.0084.v1

The objective of this investigation is therefore not to identify the pressure level required for full suppression of stick–slip by operating at excessively high supply pressures, but rather to characterize how stick–slip behavior evolves and is attenuated within the normal operating pressure range of pneumatic servo systems. Within this range, the observed trends provide meaningful insight into the role of supply pressure in governing dwell time and stick–slip dynamics, and they form a suitable basis for validating the proposed system-level friction model.

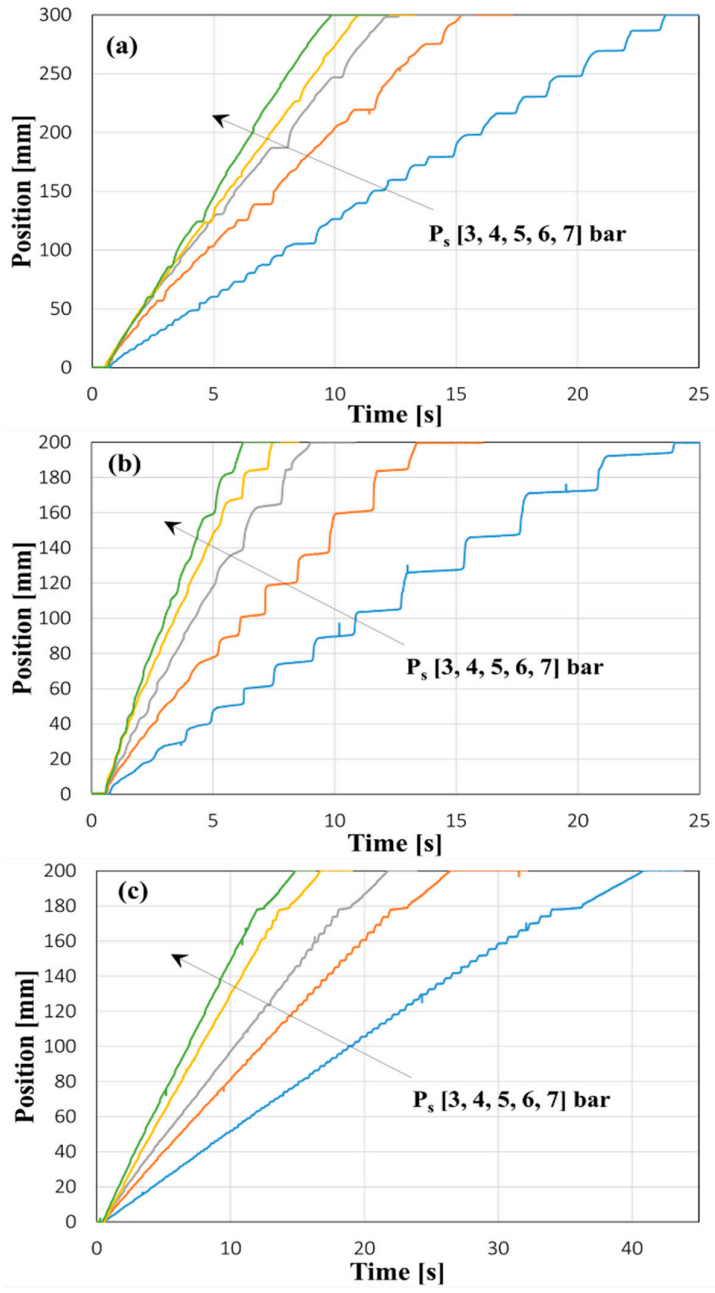

Figure 8. Effects of air source pressure on stick-slip motion (outstroke): cylinder 1, b) cylinder 2, c) cylinder 3.

4.1.4. Effects of External Load

Figure 9 shows the effect of external load on the stick–slip motion of Cylinder 1, with the load mass varied from 0.2 kg to 5.3 kg while keeping the supply pressure and valve control signal constant. Stick–slip behavior is observed at all investigated load levels, and the piston motion consistently exhibits a step-like profile throughout the entire stroke.

 doi:10.20944/preprints202604.0084.v1

As the external load increases, the overall number of stick–slip cycles within one stroke remains nearly unchanged. However, the displacement associated with each slipping event increases gradually with load, resulting in larger step heights for higher load masses. Consequently, the total time required for the piston to complete its stroke decreases slightly at higher loads, despite the persistence of stick–slip motion.

These observations indicate that external load does not significantly alter the mechanism responsible for stick–slip occurrence, which is primarily governed by pressure build-up during the sticking phase and pressure loss during slipping due to air compressibility. Instead, an increased load mainly affects the dynamic response of the piston once sliding is initiated. A higher inertial force allows the piston to travel a longer distance after overcoming static friction, leading to larger slip amplitudes, while the pressure build-up process preceding each slip remains largely unchanged.

From a system-level perspective, these results suggest that external load acts as a secondary factor that modulates the manifestation of stick–slip motion rather than its fundamental origin. Compared with airflow rate and supply pressure, which strongly influence dwell time through pneumatic dynamics, changes in external load primarily influence the slipping phase without substantially affecting the sticking phase. This behavior is consistent with the modeling framework presented in Section 3, where load affects the mechanical dynamics but does not directly modify the pressure accumulation process governing stick–slip initiation.

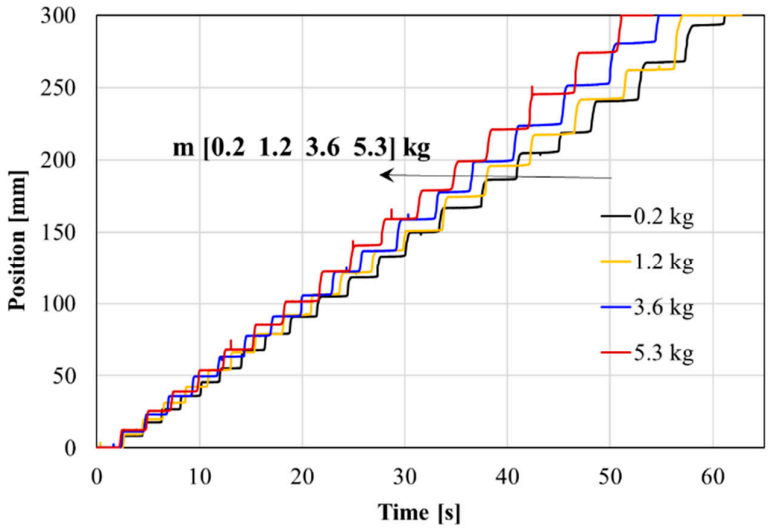

Figure 9. Effect of external load on stick-slip motion of Cylinder 1 (p_s=4 bar, u=0.3 V).

4.1.5. Effect of Initial Piston Position

Figure 10 illustrates the influence of the initial piston position on stick–slip motion for the three pneumatic cylinders. Different initial positions along the cylinder stroke are considered while keeping the airflow rate, supply pressure, and external load constant. For all cylinders and all examined initial positions, stick–slip motion is consistently observed, indicating that the initial piston position does not eliminate the occurrence of stick–slip. A pronounced effect of the initial piston position can be observed in the first stick–slip cycle. When the piston starts from a larger initial position, corresponding to a larger initial chamber volume, the piston remains stationary for a longer period before the first slipping event occurs. This manifests as an increased dwell time at the beginning of motion, which is clearly visible in all three subfigures. The increase in initial dwell time reflects the longer time required for compressed air to accumulate sufficient pressure in a larger volume to overcome static friction.

 doi:10.20944/preprints202604.0084.v1

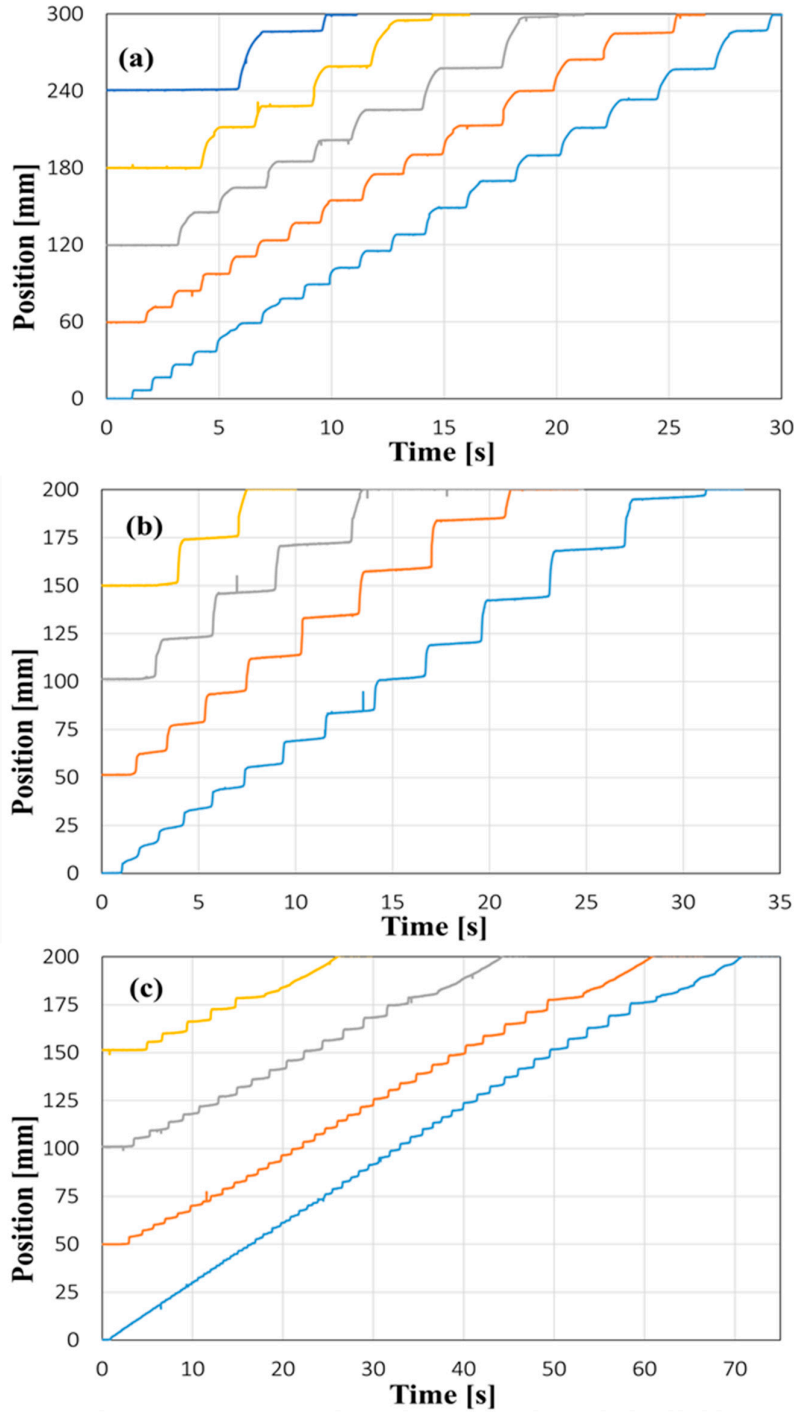

Figure 10. Effects of the initial position of the piston on stick-slip phenomenon: a) cylinder 1, b) cylinder 2, c) cylinder 3.

After the first slipping event, the subsequent stick–slip cycles exhibit similar step-like characteristics regardless of the initial piston position. The number of stick–slip cycles, the approximate dwell time between successive slips, and the slip amplitudes remain largely unchanged once the piston has started moving. This indicates that the influence of the initial piston position is primarily confined to the early stage of motion and does not significantly alter the underlying stick–slip mechanism during steady progression along the stroke.

 doi:10.20944/preprints202604.0084.v1

From a system-level perspective, these results highlight the role of initial chamber volume in determining the transient pressure build-up required to initiate motion, while confirming that the recurring stick–slip behavior during subsequent motion is governed by the local balance between airflow-induced pressure accumulation, pressure loss due to volume expansion, and friction. This observation is fully consistent with the system equations in Section 3, where chamber volume directly affects pressure dynamics but does not modify the friction law itself.

4.2. Simulation Results

This section shows comparisons between the stick-slip characteristics measured for all three cylinders and those simulated using the system model in Section 3. The simulations were performed using MATLAB/Simulink software, employing a numerical Runge-Kutta method with a step size of 0.0016 seconds to solve the differential equations. The input conditions, such as valve control signals, supply air pressure, and external load, were consistent with those used in the experiments. The parameters of the pneumatic servo system and the friction models are detailed in Table 2.

Simulation results obtained using the system-level model are compared with experimental measurements for the three pneumatic cylinders. For each cylinder, simulations are conducted for one representative operating condition corresponding to the experimental cases shown in Figures 11–13. Two friction models are considered: the revised LuGre (RLG) friction model with constant static friction and the proposed model incorporating dwell-time-dependent static friction.

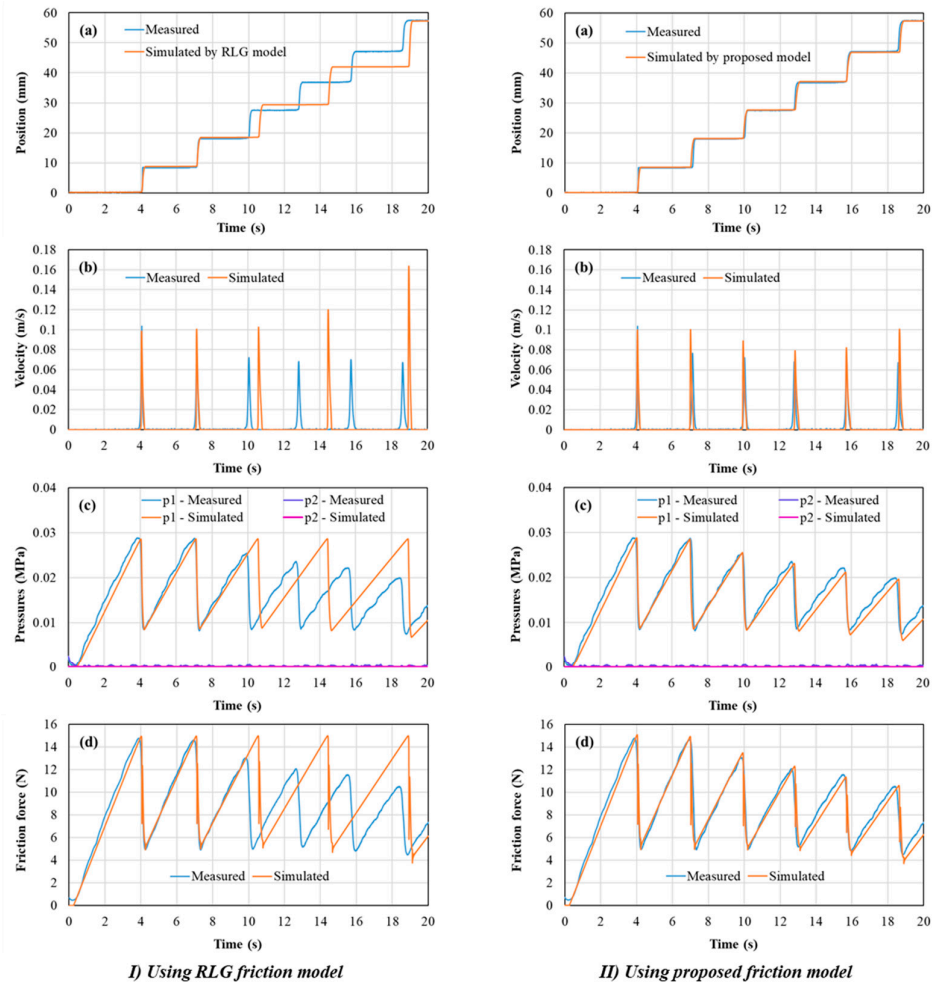

Figure 11. Comparison of experimental and simulation results for Cylinder 1: a) piston position, b) piston velocity, c) pressures p_1 and p_2, d) friction force.

 doi:10.20944/preprints202604.0084.v1

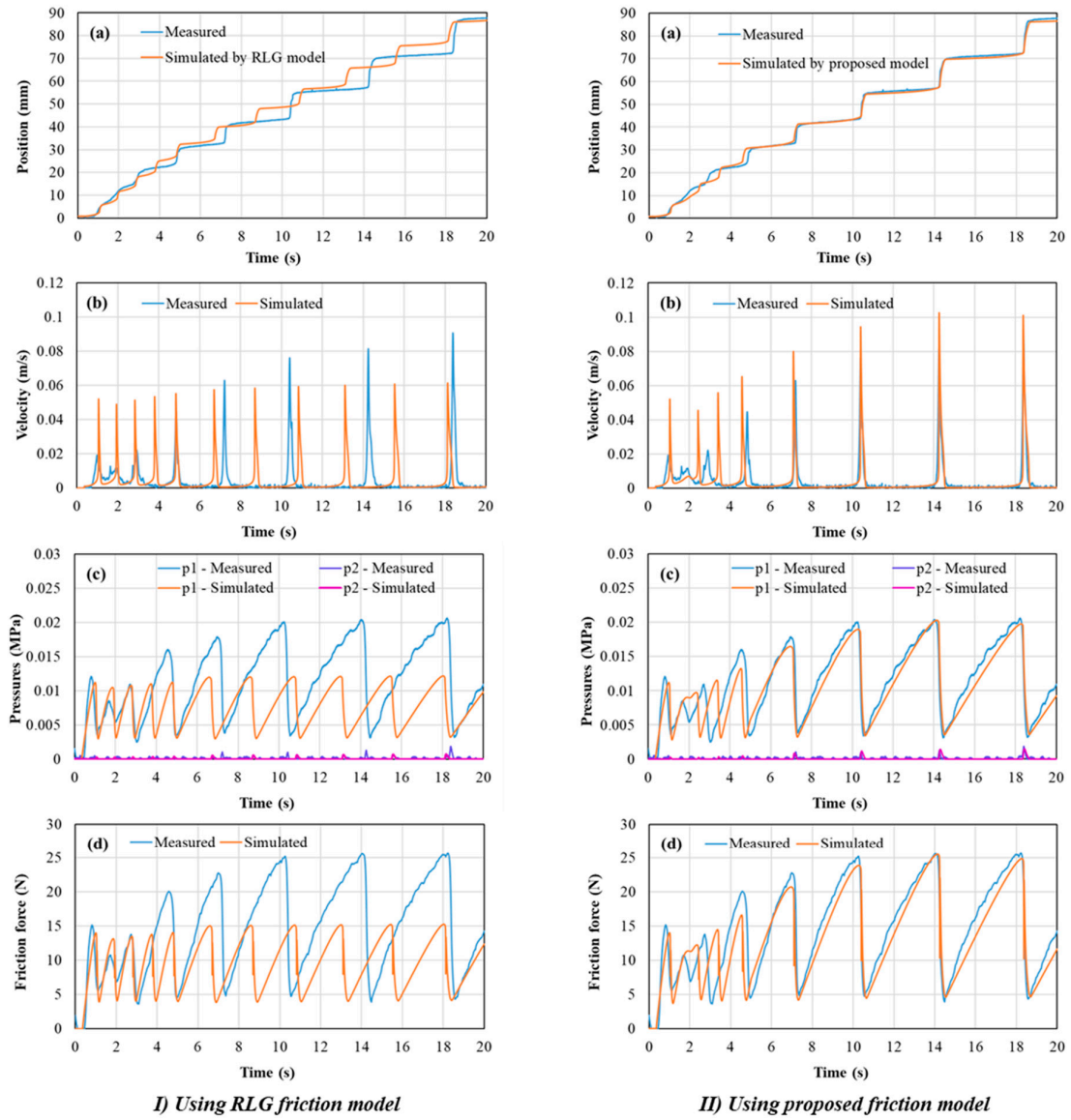

Figure 12. Comparison of experimental and simulation results for Cylinder 2: a) piston position, b) piston velocity, c) pressures p_1 and p_2, d) friction force.

For all three cylinders, the simulations using the RLG friction model can reproduce the general trend of piston motion and capture the first one or two stick–slip cycles. However, as the motion progresses, the RLG-based simulations deviate noticeably from the experimental observations. In particular, the RLG model fails to reproduce the correct number of stick–slip cycles and does not capture the gradual variation of dwell time, pressure peaks, and friction force observed in the experiments. This limitation becomes especially evident for Cylinder 3, where frequent short stick–slip cycles persist throughout the entire stroke.

In contrast, the proposed model incorporating dwell-time-dependent static friction exhibits significantly improved agreement with experimental results for the representative cases considered. The model successfully reproduces the persistence of stick–slip motion and its gradual attenuation, as well as the evolution of pressure and friction force over successive cycles. For Cylinder 3, the proposed model captures the experimentally observed micro stick–slip behavior with short dwell times and small slip amplitudes, which is not adequately represented by the RLG model.

 doi:10.20944/preprints202604.0084.v1

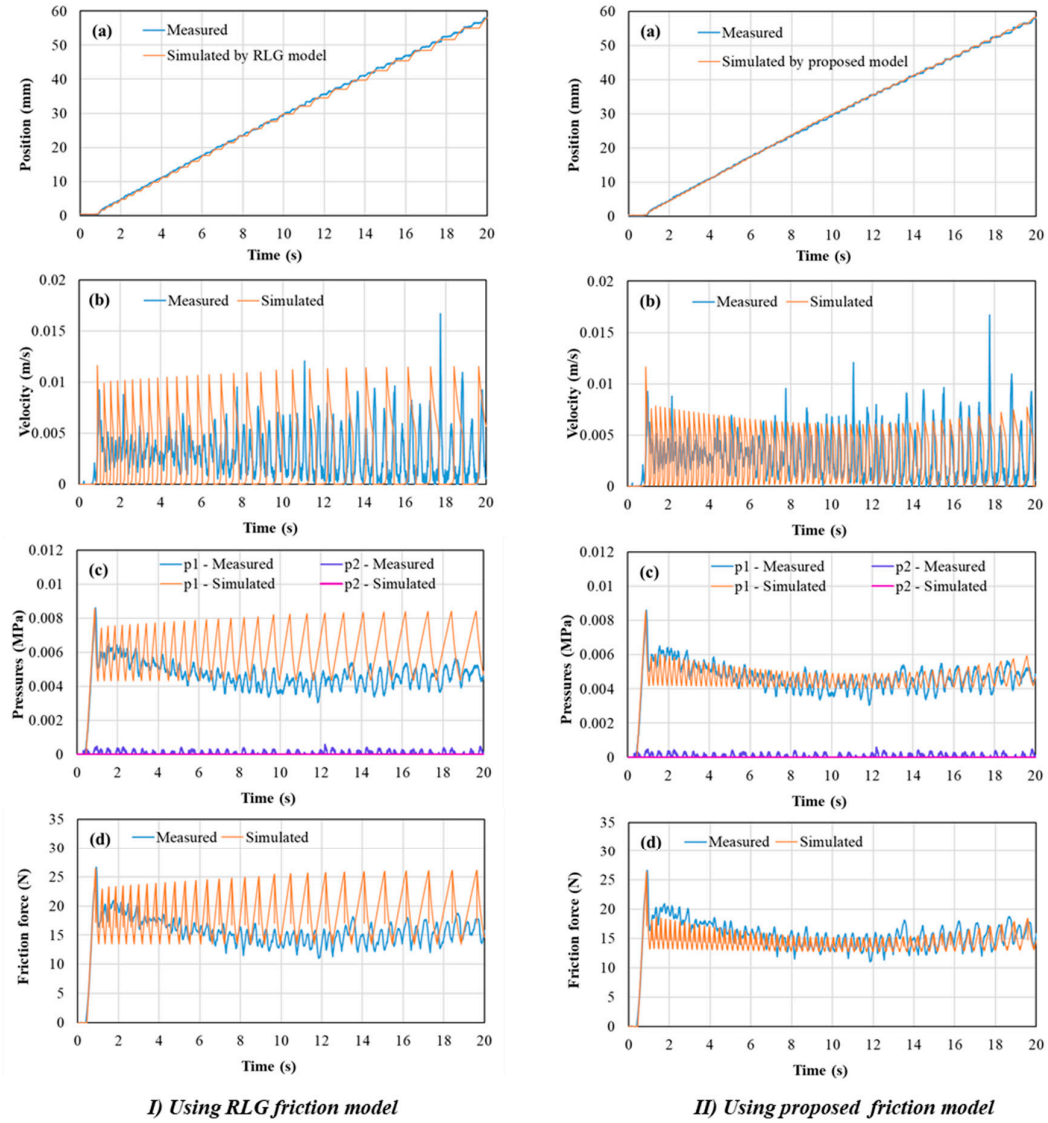

Figure 13. Comparison of experimental and simulation results for Cylinder 3: a) piston position, b) piston velocity, c) pressures p_1 and p_2, d) friction force**.**

It should be emphasized that the improvement in simulation results is not achieved by tuning friction force levels for different operating conditions. Instead, it results from incorporating the dwell time generated by the system dynamics into the friction evolution. In the proposed model, the dwell time arises naturally from the coupled interaction between airflow, pressure build-up, air compressibility, and piston motion, and the static friction force is updated accordingly. This mechanism allows the model to reflect the history-dependent behavior observed experimentally, even when simulations are performed for a single operating condition per cylinder.

The purpose of the simulation study is therefore not to provide a comprehensive parametric validation of the model under all operating conditions, but to verify that the proposed dwell-time-dependent friction formulation can reproduce the key mechanisms governing stick–slip motion observed experimentally. The close agreement between experiments and simulations for the representative cases demonstrates that the proposed model captures the essential physics of pneumatic stick–slip dynamics and provides a sound basis for further parametric studies and control-oriented investigations.

 doi:10.20944/preprints202604.0084.v1

Table 2. System parameters used in simulation.

Parameters	Values		
	Cylinder 1	**Cylinder 2**	**Cylinder 3**
A_1 (m^2)	4.91×10^{-4}	13×10^{-4}	31×10^{-4}
A_2 (m^2)	4.12×10^{-4}	11×10^{-4}	28×10^{-4}
V_{10} (m^3)	3×10^{-5}	5×10^{-5}	7×10^{-5}
V_{20} (m^3)	10×10^{-5}	10×10^{-5}	10×10^{-5}
M (kg)	0.45	0.65	0.98
L (m)	0.3	0.2	0.2
F_{smax} (N)	15.45	22	26
F_c (N)	4	0.5	3
v_s (m/s)	0.012	0.033	0.003
v_b (m/s)	0.05	0.05	0.05
n	2.5	2.5	2.5
σ_2 (Ns/m)	85	210	350
σ_1 (Ns/m)	0.1	0.1	0.1
τ_{hp} (s)	0.01	0.013	0.016
τ_{hn} (s)	0.32	0.3	0.28
τ_{h0} (s)	36	38	42
α	0.45	0.55	0.62
γ	0.22	0.43	0.18
K_{V1} (m^2/V)	4.8×10^{-8}		
K_{V2} (m^2/V)	1×10^{-6}		
T (^0K)	300		
k	1.3997		
u_m (V)	2.65		
u_n (V)	2.35		
p_{atm} (N/m^2)	1×10^5		

5. Conclusions

This paper investigated the stick–slip characteristics of pneumatic cylinders operating at low velocities through combined experimental measurements and system-level modeling. Experiments conducted on three different pneumatic cylinders demonstrated that stick–slip motion persists over a wide range of practical operating conditions and can manifest in different forms, ranging from pronounced stick–slip with long dwell times to frequent micro stick–slip with very small slip amplitudes. Variations in airflow rate and air source pressure were shown to gradually attenuate stick–slip behavior rather than eliminate it, while external load mainly influenced slip amplitude and the initial piston position primarily affected the first sticking phase.

The experimental results confirmed that stick–slip behavior in pneumatic cylinders is governed by a nonlinear interaction between air compressibility, pressure build-up and loss, piston motion, and friction, rather than by friction characteristics alone. Based on these observations, a comprehensive system-level mathematical model of a pneumatic servo system was developed. The revised LuGre (RLG) friction model was adopted as the baseline framework, and a dwell-time-dependent static friction formulation was introduced to account for the experimentally observed evolution of static friction during repeated stick–slip cycles.

 doi:10.20944/preprints202604.0084.v1

Numerical simulations were performed for representative operating conditions for each tested cylinder. While simulations based on the RLG friction model were able to reproduce the initial stick–slip cycles, they failed to capture the persistence and progressive evolution of stick–slip motion observed experimentally. In contrast, the proposed model incorporating dwell-time-dependent static friction successfully reproduced key features of the measured stick–slip behavior, including the duration of sticking phases, the number of stick–slip cycles, and the evolution of pressure and friction force.

Within this scope, the proposed model provides a physically consistent system-level framework for analyzing stick–slip dynamics under practical operating conditions. The modeling approach developed in this study offers a useful basis for future parametric investigations and control-oriented strategies aimed at improving low-speed motion performance in pneumatic servo systems.

Author Contributions: Conceptualization, B.T.X.; methodology, B.T.X. and H.N.N.; Simulation and experimental validation, H.N.N. and P.P.P.; formal analysis, B.T.X. and H.N.N.; writing—original draft preparation, H.N.N. and P.P.P.; writing—review and editing, B.T.X.; project administration and funding acquisition B.T.X. All authors have read and agreed to the published version of the manuscript.

Funding: This research was funded by the Ministry of Education and Training, grant number B2024-BKA-14.

Data Availability Statement: Data are contained within the article.

Conflicts of Interest: The authors declare no conflicts of interest.

Abbreviations

The following abbreviations are used in this manuscript:

ADC	Analog-to-Digital Converter
DAC	Digital-to-Analog Converter
RLG	Revised LuGre (Friction Model)

References

1. Pratt, T.K.; Williams, R. Non-linear analysis of stick–slip motion. *J. Sound Vib.* **1981**, *74*, 531–542.
2. Armstrong-Helouvry, B. *Control of Machines with Friction*; Springer: Boston, MA, USA, 1991.
3. Armstrong-Helouvry, B.; Dupont, P.; Canudas de Wit, C. A survey of models, analysis tools and compensation methods for the control of machines with friction. *Automatica* **1994**, *30*, 1083–1138.
4. Hamiti, K.; Voda-Besançon, A.; Roux-Buisson, H. Position control of a pneumatic actuator under the influence of stiction. *Control Eng. Pract.* **1996**, *4*, 1079–1088.
5. Pai, K.R.; Shih, M.C. Nanoaccuracy position control of a pneumatic cylinder driven table. *JSME Int. J. Ser. C* **2003**, *46*, 1062–1067.
6. Renn, J.C.; Liao, C.M. A study on the speed control performance of a servo-pneumatic motor and its application to pneumatic tools. *Int. J. Adv. Manuf. Technol.* **2004**, *23*, 572–576.
7. Saravanakumar, D.; Mohan, B.; Muthuramalingam, T. A review on recent research trends in servo pneumatic positioning systems. *Precis. Eng.* **2017**, *49*, 481–492.
8. Tokashiki, R.; Fujita, T.; Kagawa, T. Stick–slip motion in pneumatic cylinders driven by meter-out circuit. *Trans. Jpn. Hydraul. Pneumat. Soc.* **2000**, *31*, 170–175.
9. Zhang, B.H.; Ma, Y.F.; Cheng, H.F.; Peng, G.Z. A new method to predict the occurrence of stick–slip in pneumatic cylinders. In *Proceedings of the JFPS International Symposium on Fluid Power*; Tsukuba, Japan, 7–10 November 2005; Volume 6, pp. 812–816.
10. Fan, W.; Liu, Q.; Zhang, B.; Peng, G. Study on the stick–slip criterion of unsymmetrical cylinder driven by meter-out circuit. In *Proceedings of the IEEE International Conference on Mechatronics*; Kumamoto, Japan, 2007; pp. 1–5.
11. Brun, X.; Sesmat, S.; Thomasset, D.; Scavarda, S. Study of the "sticking and restarting phenomenon" in electropneumatic positioning systems. *J. Dyn. Syst. Meas. Control* **2005**, *127*, 173–184.

 doi:10.20944/preprints202604.0084.v1

12. Azzi, A.; Maoui, A.; Fatu, A.; **et al.** Experimental study of friction in pneumatic seals. *Tribol. Int.* **2019**, *135*, 432–443.
13. Qian, P.F.; Tao, G.L.; Chen, J.F.; **et al.** Modeling and simulation of stick–slip motion for pneumatic cylinders based on meter-in circuit. *Appl. Mech. Mater.* **2011**, *130–134*, 775–780.
14. Canudas de Wit, C.; Olsson, H.; Åström, K.J.; Lischinsky, P. A new model for control of systems with friction. *IEEE Trans. Autom. Control* **1995**, *40*, 419–425.
15. Tran, X.; Dao, H.; Tran, K. A new mathematical model of friction for pneumatic cylinders. *Proc. Inst. Mech. Eng. Part C J. Mech. Eng. Sci.* **2016**, *230*, 2399–2412.
16. Tran, X.B.; Nguyen, V.L.; Tran, K.D. Effects of friction models on simulation of pneumatic cylinders. *Mech. Sci.* **2019**, *10*, 517–528.
17. Liu, Y.F.; Li, J.; Zhang, Z.M.; Hu, X.H.; Zhang, W.J. Experimental comparison of five friction models on the same test bed of micro stick–slip motion systems. *Mech. Sci.* **2015**, *6*, 15–28.
18. Dahl, P.R. *A Solid Friction Model*; The Aerospace Corporation: El Segundo, CA, USA, 1968.
19. Dupont, P.; Hayward, V.; Armstrong, B.; Altpeter, F. Single-state elastoplastic friction models. *IEEE Trans. Autom. Control* **2002**, *47*, 787–792.